

1

2 VANESSA E RUBIO (Orcid ID : 0000-0003-4912-0794)

3 DR JENNY ZAMBRANO (Orcid ID : 0000-0002-0122-9937)

4 MS MARÍA NATALIA UMAÑA (Orcid ID : 0000-0001-5876-7720)

5 DR NATHAN SWENSON (Orcid ID : 0000-0003-3819-9767)

6

7

8 Article type : Research Article

9

10

11 Handling Editor: Julieta Rosell

12

13 **Improving predictions of tropical tree survival and growth by incorporating**
14 **measurements of whole leaf allocation**

15

16

17 Vanessa E. Rubio¹, Jenny Zambrano², Yoshiko Iida³, María Natalia Umaña⁴, and Nathan
18 G. Swenson¹

19

20 ¹Department of Biology, University of Maryland, College Park, Maryland 20742, U.S.A.

21

22 ²The School of Biological Sciences, Washington State University, Pullman, WA 99164,
23 U.S.A

24

25 ³Forestry and Forest Products Research Institute, Matsunosato 1, Tsukuba 3058687,
26 Japan

27

28 ⁴Department of Ecology and Evolutionary Biology, University of Michigan, Ann Arbor,
29 Michigan, 48109, U.S.A. maumana@umich.edu

This is the author manuscript accepted for publication and has undergone full peer review but has not been through the copyediting, typesetting, pagination and proofreading process, which may lead to differences between this version and the [Version of Record](#). Please cite this article as [doi: 10.1111/1365-2745.13560](https://doi.org/10.1111/1365-2745.13560)

This article is protected by copyright. All rights reserved

30

31

32 Corresponding Author:

33 Vanessa E. Rubio

34 Department of Biology

35 University of Maryland

36 College Park, MD, 20742

37 vrubio@terpmail.umd.edu

38

39

40

41

42

43

44

45

46

47

48

49

50

51

52

53

54

55

56

57

58

59 **Abstract**

60 1. Individual-level demographic outcomes should be predictable upon the basis of traits.
61 However, linking traits to tree performance has proven challenging likely due to a failure
62 to consider physiological traits (i.e., hard-traits) and the failure to integrate organ-level
63 and whole plant-level trait information.

64 2. Here, we modeled the survival rate and relative growth rate of trees while considering
65 crown allocation, hard-traits, and local-scale biotic interactions, and compared these
66 models to more traditional trait-based models of tree performance.

67 3. We found that an integrative trait, total tree-level photosynthetic mass (estimated by
68 multiplying specific leaf area and crown area) results in superior models of tree survival
69 and growth. These models had a lower AIC than those including the effect of initial tree
70 size or any other combination of the traits considered. Survival rates were positively
71 related to higher values of crown area and photosynthetic mass, while relative growth
72 rates were negatively related to the photosynthetic mass. Relative growth rates were
73 negatively related to a neighbourhood crowding index. Furthermore, none of the hard-
74 traits used in this study provided an improvement in tree performance models.

75 4. *Synthesis*. Overall, our results highlight that models of tree performance can be greatly
76 improved by including crown area information to generate a better understanding of plant
77 responses to their environment. Additionally, the role of the hard-traits in improving
78 models of tree performance is likely dependent upon the level of stress (e.g. drought
79 stress), micro-environmental conditions, or short-term climatic variations that a particular
80 forest experiences.

81 **Key Words:** Community Ecology, Demographic Rate, Forest Ecology, Functional Trait,
82 Trait Integration

83 **Introduction**

84 Variation in individual performance (i.e., survival and growth) determines the structure
85 and dynamics of natural populations and communities. Differential performance is
86 largely determined by the interaction between the individual phenotype and the abiotic
87 and biotic environment (Arnold,1983; McGill, Enquist, Weiher & Westoby 2006).
88 Ecologists have linked commonly-measured morphological and physiological traits,
89 known as functional traits, to demographic rates, to facilitate predictive models of
90 populations and communities into the future.

91 There is a core suite of functional traits widely measured in plant ecology. These
92 include specific leaf area (SLA), maximum height, wood density and seed mass. These
93 traits are often referred to as “soft-traits” due to their relative ease of measurement across
94 many individuals and species and because they are, typically, indirectly related to a
95 physiological rate or life-history tradeoff of interest (Westoby, 1998; Hodgson, Wilson,
96 Hunt, Grime, & Thompson, 1999). These soft-traits are those most commonly used in
97 tree demographic models (Poorter *et al.* 2008; Wright *et al.* 2010). Maximum height
98 (Westoby, 1998; Bazzaz, Ackerly & Reekie, 2000; Westoby, Falster, Moles, Vesk &
99 Wright, 2002; Poorter, Bongers, Sterck & Wöll, 2005), wood density (Enquist, West,
100 Charnov & Brown, 1999; Chave *et al.* 2009), and seed mass (Rees, 1996; Westoby,
101 1998) typically explain the greatest amount of variance in tree performance in tropical
102 forests when compared to leaf traits like SLA (Poorter *et al.* 2008; Wright *et al.* 2010).
103 However, forest ecologists have had variable success in linking these core commonly-
104 measured suite of functional traits to tree growth and mortality rates (Poorter *et al.* 2008;
105 Wright *et al.* 2010; Paine *et al.* 2015; Yang, Cao & Swenson, 2018; Worthy & Swenson,
106 2019; Iida & Swenson, 2020).

107 There are multiple ways in which trait-based models of tree survival and growth
108 may be improved (Yang, Cao & Swenson, 2018). These include, (i) measuring traits on
109 individuals instead of using species mean values, (ii) considering less easily-measured
110 traits, (iii) integrating leaf-level trait data into the context of whole biomass allocation,
111 and (iv) accounting for biotic interactions. The first of these possibilities has been shown
112 to be important in studies that have measured individual-level trait data on thousands of
113 individuals from tens to hundreds of co-occurring sub-tropical and tropical tree species
114 (e.g., Liu *et al.* 2016; Umaña, Zhang, Cao, Lin & Swenson, 2017). However, this
115 approach may prove impractical in many cases. Therefore, here, we focus on the
116 remaining three issues: considering less easily-measured traits (i.e. hard-traits) more
117 closely aligned with plant physiological rates, the integration of leaf-level trait data into
118 the context of whole biomass allocation, and accounting for local-scale biotic
119 interactions.

120 One way forward for trait-based predictions of tree demographic performance is
121 to measure additional traits, linked to physiological processes, beyond the core suite of

122 commonly-measured soft functional traits. Soft-traits may be strongly correlated with
123 traits that are more difficult to measure (e.g., photosynthetic rates), making them the most
124 pragmatic approach for predicting tree population and community structure and dynamics
125 (e.g., Diaz *et al.* 2004). However, soft-traits may be weakly correlated or not correlated at
126 all with important physiological rates and tradeoffs. Thus, tree survival and growth may
127 be best predicted by less commonly-measured traits. Such traits often referred to as
128 “hard-traits”, are often difficult to measure, but are more closely linked to physiological
129 processes of interest (Hodgson, Wilson, Hunt, Gime, & Thompson, 1999; Lavorel &
130 Garnier, 2002; Swenson *et al.* 2017; Yang, Cao & Swenson, 2018). For example, traits
131 directly related to water use efficiency, such as leaf carbon stable isotope composition
132 (Farquhar, O’Leary & Berry, 1982; Dawson, Mambelli, Plamboeck, Templer & Tu,
133 2002) and leaf vein length per unit area (Sack & Frole, 2006; Brodribb, Feild & Jordan,
134 2007; Sack & Scoffoni, 2013, but see Gleason *et al.* 2016), should be strongly associated
135 with individual tree performance under hydraulic stress or drought events by significantly
136 affecting photosynthetic capacity and leaf hydraulic conductance (Angert, Huxman,
137 Barron-Gafford, Gerst & Venable, 2007; Correia *et al.* 2008; Gebrekirstos, van
138 Noordwijk, Neufeldt & Mitlöhner, 2011; Sack *et al.* 2013; Iida *et al.* 2016). Thus, it is
139 crucial to determine the importance of these traits in tropical forests, in which drought
140 events are expected to increase (Chadwick, Good, Martin & Rowell, 2016). These hard-
141 trait data can be used in tree performance models and then competed against models that
142 include only soft-trait data.

143 A second potential way forward is placing organ-level trait data into a whole plant
144 allocation context. Previous work has demonstrated that tree architectural traits such as
145 crown width (Iida *et al.* 2014b) or estimates of the amount of leaf area deployed for light
146 interception (e.g., Falster, Brännström, Dieckmann, & Westoby, 2011) are valuable for
147 understanding the functional strategies of plants and/or their performance. The most
148 obvious and important starting place for accomplishing this goal is an integration of the
149 most commonly measured leaf traits, SLA (i.e., the inverse of leaf mass per area [LMA]),
150 and whole crown biomass leaf area allocation (i.e., an estimation of leaf area ratio). SLA
151 reflects a fundamental tradeoff relating resource capture, leaf investment and leaf lifespan
152 at the scale of a leaf (Reich, Walters & Ellsworth, 1997). However, individuals and

153 species vary widely in their relative allocation to whole crowns and this variation makes
154 it unlikely that SLA alone will serve as a robust predictor of tree demographic rates
155 (Yang, Cao & Swenson, 2018). Individual-level and inter-specific variation in crown
156 biomass allocation or whole plant leaf mass divided by whole plant mass have been
157 identified as critical predictors of plant growth or relative growth rate, respectively
158 (Garnier, 1991; Enquist *et al.* 2007). Despite this, a placement of leaf traits into a crown
159 context is not frequently done in the current trait-based tree growth modeling literature,
160 which likely greatly reduces our ability to predict plant performance (Yang, Cao &
161 Swenson, 2018; Yang *et al.* 2020). Thus, variables representing allocation to leaves
162 should also be considered in models of tree survival and growth and these models should
163 be compared to models lacking this information.

164 Lastly, the role of local-scale biotic interactions (e.g., competition) need to be
165 considered to understand the survival and growth responses resulting from the
166 interactions between focal trees and their neighbours. Plant performance is expected to be
167 affected by local population densities via positive or negative interactions (Pacala &
168 Silander, 1985; Chesson 2000; Uriarte *et al.* 2010). Neighbourhood models that consider
169 the density, size and distance of neighbouring trees have been increasingly used in trait-
170 based studies to determine the role of neighbourhood competition in tree community
171 structure and dynamics (e.g., Uriarte *et al.* 2010; Canham, LePage, & Coates, 2004;
172 Uriarte, Canham, Thompson, & Zimmerman, 2004; Zambrano *et al.* 2019).

173 Here, we compare models of tropical tree survival and growth that incorporate
174 traits linked to tree water use (i.e. leaf carbon isotope composition (leaf δC^{13}), leaf
175 hydraulic capacity and photosynthetic rates (i.e. leaf vein length per unit area), a measure
176 of crown area multiplied by LMA to estimate tree-level allocation to photosynthetic mass
177 (M_p), and neighbourhood crowding. In this work, we ask the following questions.

178 1) How correlated are soft-traits with hard-traits? We predict a strong positive
179 correlation between leaf traits associated with hydraulic and photosynthetic capacity
180 (e.g., Brodribb *et al.* 2007) (i.e., vein length per unit area and LMA), and between leaf
181 traits related to water use efficiency such as leaf carbon isotopic composition with
182 phosphorus concentration (Brück *et al.* 2000), and wood density (Santiago *et al.* 2004).
183 Answering this question is critical because if these two types of traits are significantly

184 correlated, it would indicate that hard-traits may not be as valuable to measure and will
185 likely not dramatically improve tree survival and growth models. 2) Does the use of an
186 estimate of total tree-level photosynthetic mass (M_p) improve model fits of tree survival
187 and growth as compared to models that do not include this information? We predict that
188 the inclusion of M_p will improve model fit as it relates to crown resource allocation of the
189 whole tree-level that ultimately affects survival and growth rates. 3) Do models of tree
190 survival and growth that include traits related to water use and photosynthetic capacity
191 (i.e., hard-traits) outperform models that include commonly measured soft-traits? We
192 expect that including hard-traits will improve tree performance models as these traits are
193 closely linked to physiological responses such as photosynthetic capacity and leaf
194 hydraulic conductance. 4) Does including the effects of neighbourhood crowding
195 improve the models of tree survival and growth? We predict strong neighbourhood
196 crowding effects on tree survival and growth, due to either competition for similar
197 resources or shared enemies reducing individual performance.

198

199 **Methods**

200 *Luquillo forest dynamics plot*

201 This study was conducted in the Luquillo Forest Dynamics Plot, a 16-ha long-term forest
202 plot located in northeast Puerto Rico (18° 20' N, 65° 49' W; LTFP). The plot, divided into
203 400 20x20m quadrats, has been censused every five years since 1990, where all free-
204 standing woody stems ≥ 1 cm in diameter at breast height (*dbh*) were identified and
205 measured (Zimmerman, 2010). The plot is located in a subtropical wet forest type with
206 *Dacryodes excelsa* (Burseraceae) and the palm *Prestoea acuminata* (Arecaceae) as the
207 most dominant species. The mean annual rainfall is 3500mm/yr and mean monthly
208 temperatures range between 21-25°C. The plot experienced severe hurricane damage in
209 1989, 1998 and 2017 due to hurricanes Hugo, Georges and Maria. The censuses used in
210 this study included only those most distant from hurricane disturbance (2005 and 2011)
211 and previous work has shown that the forest largely recovered from Hugo and Georges
212 prior to the 2005 census (Swenson *et al.* 2012)

213

214 *Functional trait measurement*

215 We used soft-trait data for 111 woody plant species that were previously collected
216 (Swenson *et al.* 2012; Umana *et al.* 2015; Swenson & Umana, 2015). These traits were
217 collected from 5 to 10 adult trees per species and included: leaf phosphorus (P;
218 percentage P of dry mass), leaf carbon (C; percentage C of dry mass) and leaf nitrogen
219 (N; percentage N of dry mass) concentration; wood specific gravity (referred to as wood
220 density WD); leaf area (LA; cm²); specific leaf area (SLA; cm² g⁻¹); maximum tree height
221 (H_{max}; m); and seed dry mass (SM; g). In addition to these traits, we also measured two
222 hard-traits related to plant hydraulics. The first was vein length per unit area (VLA; mm
223 mm⁻²) measured following the protocol described in Iida *et al.* (2016). Briefly, two leaves
224 from the outer crown per species were cut into 1x1cm squares, cleared with NaOH,
225 stained with safranin, mounted on slides and imaged at 20x magnification. Next, the
226 length of non-primary veins in the image was quantified by tracing the veins in ImageJ. A
227 VLA value for 60 of the species was generated by averaging values from 3-5 individuals
228 per species. Detailed physiological studies have shown that VLA is strongly positively
229 correlated with photosynthetic capacity (Brodribb *et al.* 2007). We also quantified leaf
230 carbon stable isotope ratios (leaf δC¹³; ‰) using leaves collected between January and
231 March 2008 (i.e. midway between censuses and during the driest part of the year). The
232 isotope analyses were conducted using mass spectrometry at the Cornell University
233 Stable Isotope Laboratory using leaves from 1-3 adult trees per species. Carbon stable
234 isotope levels are indicative of water use efficiency (Farquhar, O'Leary & Berry, 1982;
235 Dawson, Mambelli, Plamboeck, Templer & Tu, 2002) and, therefore, may indicate plant
236 performance during periods of limited water.

237

238 *Trait correlations*

239 Trait values were first log-transformed to approximate normality if their distributions
240 from the raw data were not approximately normal. Correlations between the hard-traits
241 and soft-traits were examined using Pearson's correlation coefficient. In addition, we
242 applied a principal component analysis (PCA) to all traits from the same 60 species from
243 which all trait data were available to determine trait relationships and the contribution of
244 each trait to the principal components.

245

246 *Total tree-level photosynthetic mass*

247 Total tree-level photosynthetic mass (M_p) was calculated for each individual from 17 of
 248 the 30 most common species in the plot. These 17 species account for ~56% of the
 249 individuals (excluding palm species) and 13% of the species in the plot in the 2005
 250 census. We established species-specific crown allometries from field measurements
 251 (Table S1). Specifically, we measured the stem diameter and the crown radius in two
 252 cardinal directions for 5 to 25 individuals (with dbh ranging from = 0.5cm to 56.3cm) per
 253 species to produce species-specific allometries (Eq. 1, Table S1, Figure S1; $r^2=0.66-$
 254 0.97). The species-specific M_p was obtained implementing equations (1), (2) and (3) that
 255 describe the crown area allometry in terms of individual tree crown radius as follows
 256 (Hunt 1978; Poorter 1989; Niklas & Enquist, 2001; Yang, Cao & Swenson, 2018):

257

258 $\log(\text{radius}) = \text{slope} * \log(\text{dbh}) + \text{intercept}$ Eq. (1)

259 $CA = \pi * \text{radius}^2$ Eq. (2)

260 $M_p = LMA * CA$ Eq. (3)

261

262 where *intercept* and *slope* are species-specific estimates from the \log_{10} - \log_{10} allometric
 263 regressions, and leaf mass per area (LMA) = $1/SLA$, which is related to leaf lifespan and
 264 photosynthetic rates (Reich *et al.* 1997). We estimated the M_p across all individuals (i) of
 265 each species based upon their dbh_i values and crown area (CA_i). It is important to note
 266 that this approach simplifies the estimate of M_p by making the unrealistic, but a most
 267 simple, assumption that all individuals and species have an identical leaf area index.

268

269 *Neighbourhood crowding index*

270 We examined the effects of neighbours by calculating a total Neighbour Crowding Index
 271 (NCI). The negative influence of a neighbour was calculated as follows:

272

273 $NCI_i = \sum_j \frac{dbh_j^2}{d_{ij}^2}$ Eq. (4)

274

275 The index varies as a function of the squared *dbh* of the neighbour (*j*) and an inverse
 276 function of the squared distance (*d*) of the focal tree (*i*) to the neighbour (*j*) (Canham,
 277 LePage & Coates, 2004; Uriarte, Canham, Thompson & Zimmerman, 2004). The effect
 278 was calculated within a 20-m radius around the focal tree (*i*) and summed over all
 279 neighbours. Previous studies have shown that the effects of the neighbours can be
 280 detected within a radius smaller than 20m (Hubbell 2001; Uriarte, Canham, Thompson &
 281 Zimmerman, 2004; Uriarte *et al.* 2010), and that, in this forest, the effects of NCI are
 282 consistent across different radii (5m-30m) (Zambrano *et al.* 2020). We used all 128
 283 species in the 2005 census as neighbours (*j*) and estimated NCI for all individuals (*i*) of
 284 the 17 species for the demographic models.

285

286 *Modeling tree demographic rates: including total photosynthetic mass*

287 We used census data for the same 17 non-palm species for which we had species-specific
 288 allometries including all individuals with *dbh* values greater than or equal to one. We
 289 included 17,007 individuals for the survival models and 10,538 individuals for the growth
 290 models (see Table S4 for individuals per species). We measured tree survival by
 291 determining the presence of the individual in the next census. In addition, we calculated
 292 tree relative growth rate (RGR, cm y⁻¹) as follows:

293

$$294 \quad RGR = (\ln dbh_{t+\Delta t} - \ln dbh_t) / \Delta t \quad Eq. (5)$$

295

296 where *dbh_t* is measured at a successive time steps *t* (Δt , measured in years). A value of 1
 297 was added to the observed data before log-transforming. Additionally, negative values
 298 obtained (*n* = 1056), possibly due to stem shrinkage, measurement error, or breakage,
 299 were discarded before the log-transformation. Tree survival was fitted using a binomial
 300 function while tree growth was modeled using a Gaussian function. For both survival and
 301 growth, we used generalized linear mixed effect models (*lmer* and *glmer* functions from
 302 the lme4 package in R, Bates *et al.* 2015) as follows:

303

$$304 \quad Y_{isk} = \alpha_S + \beta_S \text{Variable} + \tau_S + \tau_k \quad Eq. (6)$$

305

306 where Y_{isk} represents survival (1: alive or 0: dead) or log-transformed RGR values for
 307 each individual tree i of species S , *Variable* represents any of the following (see Model
 308 selection and assessment): dbh_{0_i} (the initial dbh in 2005), M_{p_i} (the tree-level total
 309 photosynthetic mass), CA_i (crown area) of each individual i , or LMA_S (leaf mass per area)
 310 of species S . τ_S and τ_k are random effects of differences in species S and quadrat k ,
 311 respectively. α_S is species-specific intercept and β_S are species-specific coefficients
 312 representing the effect of the parameters. Parameters were z-score standardized
 313 (subtracting the mean and dividing by the standard deviation) prior to analyses.

314

315 *Model selection and assessment*

316 First, we examined whether including M_p or any of its components, LMA_S and CA_i ,
 317 instead of dbh_i increased the quality of the tree survival and growth models by fitting one
 318 model for each variable with a similar structure (intercept and the random effects) (Eq.6;
 319 Table 2). We used three different methods to select the best model: (i) the Akaike's
 320 information criterion (AIC), (ii) Akaike weights (w_i) and (iii) Cross-Validation/loss
 321 function (C-V loss). For AIC, we used a delta-AIC threshold of 2 units (AIC differences
 322 relative to the smallest AIC value: $AIC_i - AIC_{min}$). For Akaike weights, we compared the
 323 likelihood (weight of evidence) of each model to the best model by computing their
 324 Akaike's weights (Burnham & Anderson, 2002). Lastly, for the C-V loss method we
 325 calculated the test error (loss) associated to each model (i.e., goodness of fit) by
 326 performing a 10-fold cross-validation. This approach provides a direct estimate of the test
 327 error and makes fewer assumptions about the true underlying model (James, Witten,
 328 Hastie & Tibshirani, 2013). We chose the "best model" or "best models" as the one/ones
 329 with low AIC, high Akaike weight, and low C-V loss scores. To calculate the C-V loss,
 330 the data was randomly divided into 10-folds of approximately equal size. Nine of the
 331 folds were used to train the models and the one remaining fold to test the models (James,
 332 Witten, Hastie & Tibshirani, 2013). This process was repeated ten times in which a
 333 different group was treated as the test set. For the ten folds, we calculated the averaged
 334 loss for each model (the error associated with fitting each of the models on the data). We
 335 implemented two loss functions to assess the goodness of fit of a model (i.e. model
 336 quality) by estimating its prediction error on new (i.e. test) data (Hastie, Tibshirani &

337 Friedman, 2009). For tree survival models only, we used a log-loss function (cross-
 338 entropy cost function from the package MLmetrics in R, Yan 2016) that accounts for
 339 uncertainty in the predictions. For tree growth, we calculated the Huber loss that uses a
 340 quadratic loss function for small residuals or a linear loss function when residuals exceed
 341 the minimum value of the 90th quantile (package qrmix in R, Resa, Emir & Cabrera,
 342 2017). Thus, this function avoids the effects of large outliers that make the quadratic loss
 343 less robust (Hastie, Tibshirani & Friedman, 2009). When comparing models using the
 344 loss function values, the smallest value indicates the model with higher performance
 345 when predicting unseen data. In other words, this value indicates which model can be
 346 expected to perform better on other sets of data (James, Witten, Hastie & Tibshirani,
 347 2013).

348

349 *Modeling tree demographic rates: including soft- and hard-traits*

350 Following the selection of the best predictor (M_p , LMA , CA , or dbh) of survival and
 351 growth using Eq. 6 (Table 2), we fit all different model combinations that included the
 352 selected predictors, both soft- and hard-traits, and the neighbour crowding index. The
 353 models were fit controlling for multicollinearity among traits (excluding trait
 354 combinations with Pearson's correlation coefficient $|r| \geq 0.60$) using the function *pdredge*
 355 from the package MuMIn in R (Bartoń 2018), setting:

356

$$357 \quad Y_i = \alpha_S + \beta_{1S} Variable + \beta_{2S} soft_S + \beta_{3S} hard_S + \beta_{4S} NCI_i + \tau_S + \tau_k \text{ Eq. (7)}$$

358

359 where *Variable* represents the selected parameter (M_p , CA , dbh , or LMA), $soft_S$ and $hard_S$
 360 represent all the soft- and hard-traits used at the species level S , and NCI_i represents a
 361 neighbourhood crowding index at the individual level i . The τ_S and τ_k parameters are
 362 random effects for species S and quadrat k , respectively. The α_S is a species-specific
 363 intercept, β_{1S} - β_{4S} are species-specific coefficients representing the effect of the
 364 parameters. The data were z-score standardized (subtracting the mean and dividing by the
 365 standard deviation). We performed model selection following the same methodology
 366 described above in the Model selection and assessment section.

367

368 *Model averaging*

369 When multiple models were indiscernible ($AIC_i - AIC_{\min} \leq 2$) due to similar Akaike
370 weights and C-V losses, we carried out multi-model inference to increase precision and
371 reduce bias (Burnham & Anderson, 2002). This methodology first selects a model set
372 from which model averaging is performed including model selection uncertainty from the
373 set of models. We compared the standardized coefficients to determine the relative
374 importance of the variables in the averaged model. Predicted versus observed values were
375 plotted to test the fit of the model. All the analyses were carried out with the R software
376 version 3.5.1 (R Development Core Team 2008).

377

378 **Results**

379 *Correlations between soft- and hard-traits*

380 We found positive correlations between leaf δC^{13} and leaf phosphorus concentration ($r =$
381 0.27 , $P=0.004$, $n = 105$; Figure 1a), between leaf δC^{13} and wood density ($r=-0.20$, $P=0.03$,
382 $n=105$; Figure 1b), and between VLA and leaf carbon concentration ($r = 0.45$, $P<0.001$, n
383 $= 60$; Figure 1c). No significant correlations were found between the other traits studied
384 (Table S2). In the PCA, the first three principal components (PCs) accounted for 60.2%
385 of the total variance. PC1 accounted for 27.8% of the total variance and was possibly
386 related to resource capture. At the negative end of this axis, we found species with high
387 leaf phosphorus and nitrogen concentrations, and low wood density, while the positive
388 end had species with low values of leaf phosphorus and nitrogen concentrations, and high
389 wood density. The PC2 accounted for 18.4% of the total variance and was possibly
390 related to maximum height, with large-statured, low specific leaf area and large seeded
391 species found at positive values of this axis, while at negative values of this axis we
392 found small-statured species with high specific leaf area and small seeds. The PC3
393 accounted for 13.9% of the total variance and was possibly related to water use, with
394 species showing low values of vein length area, and leaf carbon concentration, and high
395 values of leaf δC^{13} at high values of this axis, while at negative values of this axis species
396 display high values of leaf vein length area and leaf carbon concentration, and low values
397 of leaf δC^{13} (Table S3 & Figure S2).

398

399 *Demographic models*

400 For tree survival the models that included M_p or CA , instead of LMA or dbh , showed a
401 slight improvement in the model quality (Table 2). Therefore, we fit all the different
402 combinations of tree survival models, controlling for multicollinearity among traits,
403 (models with M_p : 588; models with CA : 588) that included M_p , neighbourhood crowding,
404 and soft- and hard-traits (Table S5), and models that included CA , neighbourhood
405 crowding, and soft- and hard-traits (Table S6). We selected the models that had a $\Delta AIC \leq$
406 2 (Table 3), but since multiple models had indiscernible AIC values, and the Akaike
407 weights provided no strong evidence for a single superior model, we performed model
408 averaging (see results in Table 4). The averaged model that included total photosynthetic
409 mass (M_p) as a predictor showed that survival increases with total photosynthetic mass,
410 but the other traits were not significantly related to survival (Figure 2a & Table 4). The
411 averaged model that included crown area (CA) as a predictor showed, in order of
412 importance, CA , carbon concentration, maximum height, and leaf phosphorus
413 concentration as significant predictors of tree survival, with survival increasing with CA
414 and maximum height, and decreasing with leaf carbon and phosphorus concentrations
415 (Figure 2b & Table 4). Leaf nitrogen concentration, seed mass, vein length per unit area,
416 neighbourhood crowding, leaf δC^{13} , leaf area, and wood density showed low support and
417 no statistical significance. In addition, the observed versus predicted plots (Figure S3)
418 showed no difference between the survival averaged models with M_p and CA suggesting
419 that both models perform equally well.

420 For tree growth, the model that included M_p instead of its components (LMA , CA ,
421 or dbh) showed an improvement in the model quality as evidenced by a reduction in both
422 AIC and the C-V loss (Table 2). The inclusion of soft- and hard-traits and the
423 neighbourhood crowding information in growth models resulted in two models with
424 indiscernible AICs that included M_p , wood density, and neighbourhood crowding as
425 strong predictors of tree growth (Table 5). The averaged growth model showed that tree
426 growth decreases with high values of M_p , wood density, and neighbourhood crowding
427 (Figure 3 & Figure S4, Table 6). Similar to survival models, none of the tree growth
428 models with indiscernible AIC or $|r| < 0.6$ for tree relative growth rate included leaf δC^{13}
429 or vein length area as independent variables at a significance level of 0.05.

430

431 **Discussion**

432 Modeling individual-level performance including trait information is a key goal in
433 ecology (e.g., Poorter *et al.* 2008; Iida *et al.* 2014a; Paine *et al.* 2015; Iida *et al.* 2016). It
434 has been suggested that tree survival and growth models may be improved by integrating
435 leaf-level traits with whole plant allocation to leaf area, through the measurement of less
436 commonly-measured traits more directly linked to physiological rates, and the inclusion
437 of local-scale biotic interactions (Yang, Cao & Swenson, 2018). Here, we have shown
438 that growth models that integrate leaf-level traits (i.e., 1/SLA) with whole tree crown
439 allocation were superior to models that did not include crown information. Similarly,
440 survival models that integrate leaf-level traits with whole tree crown allocation or total
441 crown area were superior to models that did not include them. Surprisingly, less
442 commonly-measured traits (hard-traits), such as leaf δC^{13} and leaf vein length per area,
443 were not better predictors of tree survival and growth compared to traits widely measured
444 in plant ecology. In addition, neighbourhood crowding showed a strong effect on tree
445 growth, but not tree survival. In the following, we discuss our key results in more detail.

446

447 *How are soft-traits with hard-traits correlated?*

448 Plant ecologists often utilize easily-measured functional traits in their research to estimate
449 key tradeoffs relating to organismal form and function. These traits are referred to as soft-
450 traits, which are contrasted with hard-traits that are potentially more directly tied to
451 physiological rates and performance, but less easily measured. Thus, trait-based analyses
452 of plant performance may be strengthened by the measurement of hard-traits, but this
453 may largely hinge on the degree of correlation between soft- and hard-traits. Our results
454 showed little to no correlation between the hard-traits measured (leaf δC^{13} , vein length
455 per area (VLA)) and commonly-measured soft-traits (wood density, maximum tree
456 height, seed mass, leaf nitrogen concentration, leaf phosphorus concentration, leaf carbon
457 concentration, leaf area and specific leaf area (SLA)) (Table S2). The only exceptions
458 were correlations found between leaf δC^{13} with leaf phosphorus concentration, and with
459 wood density, and VLA with leaf carbon concentration (Figure 1, Table S2). A positive
460 relationship between leaf δC^{13} and leaf phosphorus concentration has been previously

461 described in other tropical forests (e.g., Baraloto *et al.* 2010). High values of soil
462 phosphorus, which directly determine leaf phosphorus concentration (Wright *et al.* 2004),
463 have been shown to increase plant water use efficiency (e.g., glasshouse experiment by
464 Brück *et al.* 2000; Tibetan plateau by Song *et al.* 2010; and Canadian prairies by Kröbel
465 *et al.* 2012), which corresponds with less negative values of leaf δC^{13} . Contrary to our
466 expectations, the weak negative relationship between leaf δC^{13} and wood density could
467 be explained by a decoupling of stem and leaf hydraulic traits in this forest (but see
468 Santiago *et al.* 2004 for scaling of these traits). A positive correlation between VLA and
469 leaf carbon concentration, highlighting the role of VLA with respect to within-leaf
470 support investment and not only its relation with hydraulics, has been reported previously
471 (Niinemets *et al.* 2007). Leaf veins are composed of xylem and phloem cells (Sack &
472 Scoffoni 2013), which contain mainly lignin, cellulose, and other structural
473 carbohydrates. Thus, an increase in the number of veins per unit area should be
474 associated with an increase in the amount of lignin in the leaf, which coincides with the
475 concentrations of total carbon (Poorter & Villar, 1997).

476 The negligible correlations between hard-traits with soft-traits in our study
477 suggest that the soft-traits measured here are insufficient proxies of VLA and leaf δC^{13} .
478 Nevertheless, it is possible that the strength of the correlations shown here, and the
479 importance of these hard-traits for modeling plant performance would be different if we
480 included ontogenetic differences (Grime *et al.* 1997; Poorter *et al.* 2008; Wright *et al.*
481 2010), considered another set of species (Sack *et al.* 2013), or focused on a period time
482 after intense drought events given the association of these hard-traits with tree
483 performance under hydraulic stress.

484
485 *Total tree-level photosynthetic mass and crown area as better predictors of tree*
486 *performance*

487 Studies that have only considered leaf-level traits such as SLA (e.g., Wright *et al.* 2010;
488 Paine *et al.* 2015) on large organisms (e.g., trees) likely have a reduced capacity to
489 predict demographic rates due to individual- and species-level variation in overall crown
490 allocation and architecture. Instead, total photosynthetic mass (M_p), as others have
491 proposed (e.g., Hunt, 1978; Poorter, 1989; Garnier, 1991; Enquist *et al.* 2007; Yang, Cao

492 & Swenson, 2018) should be a stronger predictor of plant survival and growth than SLA.
493 By estimating M_p via measurements of crown area integrated with LMA (i.e. $1/SLA$), we
494 generated stronger models of tree demographic rates than those including initial dbh
495 (Table 2).

496 The fact that survival models including crown area and models including total
497 photosynthetic mass performed similarly suggests that omitting LMA and measuring
498 crown area alone would be sufficient to improve the predictions of tree survival in this
499 forest (Table 3 & Figure S3). This result highlights the importance of individual-level
500 measurements (i.e., crown area, leaf area index) for improving predictions of tree
501 performance (Poorter *et al.* 2008; Wright *et al.* 2010; Yang, Cao & Swenson, 2018; Yang
502 *et al.* 2020; Iida & Swenson, 2020). It is also important to note the negative effect of M_p
503 on growth. This result could be driven by big trees, expected to have big canopies,
504 growing slower, or by variations in individual crown depths not included in this study.

505
506 We note that our estimates of M_p are still crude in that they do not consider overall
507 crown volume and measurements of the leaf area index, but they do provide a marked
508 improvement of the traditional paradigm of relating leaf-level traits to demographic rates
509 without context relating to crown allocation. It is, potentially, also important to note that
510 the impact of M_p (reduced AIC, included in all the best models, and high variable
511 importance/significance) in our models was large relative to that gained by adding or
512 removing soft- and hard-traits (see below, Table 2, Table 3 & Table 5). Thus, future work
513 should start from a foundation of crown measurements in models of tree demographic
514 rates.

515 *Hard-traits did not improve model predictions of tree survival and growth*

516 Contrary to our expectations, soft-traits were better predictors of tree performance than
517 hard-traits related to water use. These soft-traits have been found to be related to tree
518 survival and growth in other tropical forests (e.g. Enquist, West, Charnov & Brown,
519 1999; Poorter *et al.*, (2008); Chave *et al.* 2009; Wright *et al.*, (2010)). In a study of five
520 neotropical forests, Poorter *et al.*, (2008) found that wood density was the best predictor
521 of relative growth rates while survival rates increased with maximum height. Using the
522

523 forest plot used in this study, Uriarte *et al.* (2010) found that models in which the effects
524 of neighbourhood interactions were scaled to trait values such as wood density provided
525 stronger predictions of tree performance. Similarly, Zambrano *et al.* (2020) found that
526 maximum height and leaf phosphorus concentration influenced the strength (positively
527 and negatively, respectively) of neighbourhood interactions on survival rates.

528 Several explanations can be attributed to the limited model improvement when
529 adding hard-traits. One potential, but unlikely, reason is that water-related traits are not
530 an important predictor of performance. These traits are expected to be strongly associated
531 with individual performance under hydraulic stress or drought events, but they might not
532 be critical for tree performance during periods lacking intense dry events (such as the
533 period evaluated in this study: 2005-2011). Rather, these water-related traits may be more
534 important in the context of future drought events or in other forests experiencing strong
535 droughts (Chadwick, Good, Martin & Rowell, 2016; Santiago *et al.* 2018). A second
536 possibility is that these traits must be considered in light of more contextual information
537 regarding regional-to-local scale abiotic gradients (Zambrano, Marchand, & Swenson,
538 2017; Yang, Cao & Swenson, 2018). A third possibility that we consider to be the most
539 probable is that these hydraulic traits can be sensitive to micro-environmental conditions
540 or short-term climatic variations and they may need to be measured at those scales
541 (Correia *et al.* 2008; Seibt, Rajabi, Griffiths & Berry, 2008; Baraloto *et al.* 2010; Paine *et*
542 *al.* 2015). Thus, links between leaf δC^{13} values and growth may be detected at a finer
543 temporal scale than we could assay in this study. Lastly, it could be possible that the link
544 between these hard-traits (VLA and leaf δC^{13}) and tree performance is directly influenced
545 by changes in plant allocation resulting from differences in ontogeny and tree size
546 (Gibert, Gray, Westoby, Wright, & Falster, 2016; Falster, Brännström, Dieckmann, &
547 Westoby, 2011; Iida *et al.* 2014a, 2016; Falster, Duursma, & FitzJohn, 2018). For
548 example, plant traits such as LMA are known to change as the plant grows (Wright *et al.*
549 2010) due to changes in specific-size plant requirements to allocate biomass or
550 increments on construction costs (Gibert, Gray, Westoby, Wright, & Falster, 2016; Iida &
551 Swenson, 2020). Therefore, tree survival and growth models need be further refined to
552 consider changes associated with plant ontogenetic stage or size (Falster, Duursma, &
553 FitzJohn, 2018) in order to detect significant patterns.

554 Finally, including information regarding neighbour crowding only improved the
555 quality of our tree growth models (Table 5). Increased neighbourhood crowding reduced
556 tree growth, which was consistent with previous work in this forest (Uriarte, Canham,
557 Thompson & Zimmerman, 2004; Uriarte *et al.* 2010; Zambrano *et al.* 2019; Zambrano *et*
558 *al.* 2020). Although the previously described negative impact of crowding on tree
559 survival (e.g., Weiner 1990; Hubbell *et al.* 2001), neighbourhood crowding was not a
560 strong predictor of survival in this study. Specifically, survival models including
561 neighbourhood crowding had indiscernible AIC values compared to other models (Table
562 3), but in the averaged survival models, the effect of neighbourhood crowding was
563 relatively small suggesting that removing it from the models does not impact the
564 predictions. This may be due to species responding differentially to neighbourhoods by
565 having variable effective radii (Uriarte, Canham, Thompson & Zimmerman, 2004;
566 Zambrano *et al.* 2020), or because the neighbourhood crowding index did not include
567 species-specific functional trait values (Uriarte *et al.* 2010).

568

569 **Conclusions**

570 Studies linking traits to tree performance usually fail to include physiological traits and
571 whole plant allocation information. In this study we considered the importance of hard-
572 traits, crown allocation, an integration of organ-level traits and crown allocation, and
573 biotic interactions to determine whether models of tropical tree performance could be
574 improved in comparison to models that only use easily-measured soft-traits. Given that
575 the leaf δC^{13} and VLA traits failed to improve the models and did not strongly correlate
576 with the leaf and stem traits, we suggest that soft-traits used in this study might not be
577 useful as proxies of leaf δC^{13} and VLA in this forest, and that these hard-traits might not
578 be useful without contextual information regarding water availability (i.e., drought
579 events) and/or finer scale sampling.

580 Lastly, the inclusion of a whole crown allocation data or crown area improved our
581 predictions of tree performance. This result underscores the importance of integrating
582 organ-level trait data with whole plant allocation data when modeling the performance of
583 tropical trees and how they interact with the abiotic and biotic environment. Thus, future
584 studies should strive to incorporate individual-level crown data and continue to seek out

585 additional less commonly-measured traits and biotic interactions that will improve tree
586 survival and growth models.

587

588 **Acknowledgements**

589 This work was funded by a Smithsonian ForestGeo grant and US NSF funding to NGS
590 (DEB-1545761 and DEB-1802812). We would like to thank the comments from two
591 anonymous reviewers and the editors that greatly improved this manuscript. The authors
592 thank Krittika Petprakob for comments that improved the manuscript, and Boris Ngouajio
593 for tracing the leaf images. Repeat censusing of the Luquillo Forest Dynamics Plot lead
594 by J.K. Zimmerman, N. Brokaw, M. Uriarte and J. Thompson, has been made possible by
595 these awards to the plot and Luquillo LTER (BSR-9015961, DEB-0516066, BSR-
596 88111902, DEB-9411973, DEB- 008538, DEB-0218039, and DEB-0620910) and the
597 hundreds of field workers that have collected the data.

598

599 **Authors' contributions**

600 V.E.R. and N.G.S. generated the research idea; N.G.S., Y.I. and M.N.U. organized and
601 conducted trait data collection; V.E.R. and J.Z. analyzed the data; and V.E.R. and N.G.S.
602 wrote the paper with comments from all other authors.

603

604 **Data Accessibility Statement**

605 All forest plot data are available on the Luquillo LTER data website:
606 <https://doi.org/10.6073/pasta/6061298660b4ceb806ba49805a950646>. Soft-trait data
607 available from the Dryad Digital Repository: <https://doi.org/10.5061/dryad.j2r53/1>
608 (Swenson & Umaña, 2015). Allometric relationships are provided in the supplemental
609 material. Hard-trait data available from the Dryad Digital Repository:
610 <https://doi.org/10.5061/dryad.4mw6m908c> (Swenson, Iida & Rubio, 2020). Code for this
611 study is available on <https://doi.org/10.5281/zenodo.4273902>.

612

613 **References**

- 614 Angert, A. L., Huxman, T. E., Barron-Gafford, G. A., Gerst, K. L., & Venable, D. L.
615 (2007). Linking growth strategies to long-term population dynamics in a guild of desert
616 annuals. *Journal of Ecology*, 95: 321:331. doi: 10.1111/j.1365-2745.2006.01203.x
617
- 618 Arnold, S. J. (1983). Morphology, performance and fitness. *Amer Zool* 23:347-361.
619
- 620 Baraloto, C., Paine, C. E. T., Poorter, L., Beauchene, J., Bonal, D., Domenach, A. M.,
621 ...Chave, J. (2010). Decoupled leaf and stem economics in rain forest trees. *Ecology*
622 *Letters*, 13(11), 1338–1347. doi:10.1111/j.1461-0248.2010.01517.x
623
- 624 Bartoń, K. (2018). MuMIn: Multi-Model Inference. R package version 1.42.1.
625 <https://CRAN.R-project.org/package=MuMIn>
626
- 627 Bates, D., Mächler, M., Bolker, B., & Walker, S. (2015). Fitting Linear Mixed-Effects
628 Models Using lme4. *Journal of Statistical Software*, 67(1), 1–48.
629 doi: [10.18637/jss.v067.i01](https://doi.org/10.18637/jss.v067.i01).
630
- 631 Bazzaz, F. A., Ackerly, D. D., & Reekie, E. G. (2000). Reproductive Allocation in Plants.
632 In M. Fenner (Ed.), *Seeds. The ecology of regeneration in plant communities* (pp. 1–29).
633 Wallingford, UK: CAB International. doi:10.1016/B978-012088386-8/50001-6
634
- 635 Brodribb, T. J., Feild, T. S., & Jordan, G. J. (2007). Leaf Maximum Photosynthetic Rate
636 and Venation Are Linked by Hydraulics. *Plant Physiology*, 144(4), 1890–1898.
637 doi:10.1104/pp.107.101352
638
- 639 Brück, H., Payne, W. A., & Sattelmacher, B. (2000). Effects of phosphorus and water
640 supply on yield, transpirational water-use efficiency, and carbon isotope discrimination of
641 pearl millet. *Crop Science*, 40(1), 120–125. doi:10.2135/cropsci2000.401120x
642

- 643 Burnham, K.P. & Anderson, D.R. (2002) Model Selection and Inference: A Practical
644 Information-Theoretic Approach. 2nd Edition, Springer-Verlag, New York. doi:
645 10.1007/b97636
646
- 647 Canham, C. D., LePage, P. T., & Coates, K. D. (2004). A neighbourhood analysis of
648 canopy tree competition: effects of shading versus crowding. *Canadian Journal of Forest*
649 *Research*, 34, 778-787. doi: 10.1139/x03-232
650
- 651 Chadwick, R., Good, P., Martin, G., & Rowell, D. P. (2016). Large rainfall changes
652 consistently projected over substantial areas of tropical land. *Nature Climate*
653 *Change*, 6, 177–181. <https://doi.org/10.1038/nclimate2805>
654
- 655 Chave, J., Coomes, D., Jansen, S., Lewis, S. L., Swenson, N. G., & Zanne, A. E. (2009).
656 Towards a worldwide wood economics spectrum. *Ecology Letters*, 12(4), 351–366. doi:
657 10.1111/j.1461-0248.2009.01285.x
658
- 659 Chesson, P. (2000). Mechanisms of maintenance of species diversity. *Annu. Rev. Ecol.*
660 *Syst* 31: 343-366.
661
- 662 Correia, I., Almeida, M. H., Aguiar, A., Alía, R., David, T. S., & Pereira, J. S. (2008).
663 Variations in growth, survival and carbon isotope composition ($\delta^{13}\text{C}$) among *Pinus*
664 *pinaster* populations of different geographic origins. *Tree Physiology*, 28(10), 1545–
665 1552. doi:10.1093/treephys/28.10.1545
666
- 667 Dawson, T. E., Mambelli, S., Plamboeck, A. H., Templer, P. H., and Tu, K. P. (2002).
668 Stable isotopes in plant ecology. *Annual Review of Ecology and Systematics*, 33: 507-
669 559. doi: 10.1146/annurev.ecolsys.33.020602.095451
670
- 671 Díaz, S; Hodgson, J. G., Thompson, K., Cabido, M., Cornelissen, J. H. C., Jalili, A.,
672 Montserrat-Martí, G., ..., Zak, M. R. (2004). The plant traits that drive ecosystems:
673 Evidence from three continents. *Journal of Vegetation Science*, 15, 295-304.

674

675 Enquist, B. J., West, G. B., Charnov, E. L., & Brown, J. H. (1999). Allometric scaling of
676 production and life-history variation in vascular plants. *Nature*, 401(6756), 907–911.

677 doi:10.1038/44819

678

679 Enquist, B.J., A.J. Kerkhoff, S.C. Stark, N.G. Swenson, M.C. McCarthy, and C.A. Price.
680 (2007). A general integrative model for scaling plant growth and functional trait

681 spectra. *Nature* 449:218-222. doi: 10.1038/nature06061

682

683 Falster, D. S., Brännström, Å., Dieckmann, U. & Westoby, M. (2011). Influence of four
684 major plant traits on average height, leaf-area cover, net primary productivity, and

685 biomass density in single-species forests: A theoretical investigation. *Journal of Ecology*
686 99: 148-164.

687

688 Falster, D. C., Duursma, R. A., & FitzJohn, R. G. (2018). How functional traits influence
689 plant growth and shade tolerance across the life cycle. *Proceedings of the National*

690 *Academy of Sciences* 115 (29) E6789-E6798; doi: 10.1073/pnas.1714044115

691

692 Farquhar, G. D., O’Leary, M. H., & Berry, J. A. (1982). On the relationship between
693 carbon isotope discrimination and the intercellular carbon dioxide concentration in

694 leaves. *Aust. J. Plant Physiology*, 9, 121-137. doi: 10.1071/PP9820121

695

696 Garnier, E. (1991). Resource capture, biomass allocation and growth in herbaceous
697 plants. *Trends Ecol Evol* 6:126-31. doi: 10.1016/0169-5347(91)90091-B

698

699 Gebrekirstos, A., van Noordwijk, M., Neufeldt, H., & Mitlöhner, R. (2011).

700 Relationships of stable carbon isotopes, plant water potential and growth: An approach to

701 assess water use efficiency and growth strategies of dry land agroforestry species. *Trees -*

702 *Structure and Function*, 25(1), 95–102. doi:10.1007/s00468-010-0467-0

703

- 704 Gibert, A., Gray, E. F., Westoby, M., Wright, I. J., & Falster, D. S. (2016). On the link
705 between functional traits and growth rate: a meta-analysis shows effects change with
706 plant size, as predicted. *Journal of Ecology* 104, 1488-1503. Doi: 10.1111/1365-
707 2745.12594
708
- 709 Gleason, S.M., Blackman, C.J., Chang, Y., Cook, A.M., Laws, C.A. and Westoby, M.
710 (2016). Weak coordination among petiole, leaf, vein, and gas-exchange traits across
711 Australian angiosperm species and its possible implications. *Ecology and Evolution* 6,
712 267-278. doi:10.1002/ece3.1860
713
- 714 Grime, J. P., Thompson, K., Hunt, R., Hodgson, J. G., Cornelissen, J. H. C., Rorison, I.
715 H., ... Whitehouse, J. (1997). Integrated screening validates primary axes of
716 specialization in plants. *Oikos*, 79, 259-281. doi: 10.2307/3546011
717
- 718 Hastie, T., Tibshirani, R., & Friedman, J. H. (2009). *The elements of statistical learning: data mining, inference, and prediction*. 2nd ed. New York: Springer.
719
720
- 721 Hodgson, J. G., Wilson, P. J., Hunt, R., Grime, J. P., & Thompson, K. (1999). Allocating
722 C-S-R plant functional types: a soft approach to a hard problem. *Oikos*, 85, 282-294
723
- 724 Hubbell, S.P., Ahumada, J.A., Condit, R. & Foster, R.B. (2001) Local neighbourhood
725 effects on long-term survival of individual trees in a neotropical forest. *Ecological*
726 *Research*, 16, 859–875.
727
- 728 Hunt, R. (1978) *Plant Growth Analysis*. Edward Arnold Limited, London.
729
- 730 Iida, Y., Kohyama, T. S., Swenson, N. G., Su, S. H., Chen, C. T., Chiang, J. M., & Sun, I.
731 F. (2014a). Linking functional traits and demographic rates in a subtropical tree
732 community: The importance of size dependency. *Journal of Ecology*, 102(3), 641–650.
733 doi:10.1111/1365-2745.12221
734

- 735 Iida, Y., Poorter, L., Sterck, F., Kassim, A. R., Potts, M. D., Kubo, T., & Takashi, S. K.
736 (2014b). Linking size-dependent growth and mortality with architectural traits across 145
737 co-occurring tropical tree species. *Ecology*, 95(2), 353-363.
738
- 739 Iida, Y., Sun, I. F., Price, C. A., Chen, C. T., Chen, Z. S., Chiang, J. M., ..., Swenson, N.
740 G. (2016). Linking leaf veins to growth and mortality rates: an example from a
741 subtropical tree community. *Ecology and Evolution*, 6(17), 6085–6096.
742 doi:10.1002/ece3.2311
743
- 744 Iida, Y. & Swenson, N.G. (2020). Towards linking species traits to demography and
745 assembly in diverse tree communities: Revisiting the importance of size and allocation.
746 *Ecological Research*, online first. doi: 10.1111/1440-1703.12175
747
- 748 James, G., Witten, D., Hastie, T., & Tibshirani, R. (2013). *An Introduction to Statistical*
749 *Learning with Applications in R*. New York: Springer.
750
- 751 Kröbel, R., Campbell, C. A., Zentner, R. P., Lemke, R., Steppuhn, H., Desjardins, R. L.,
752 & De Jong, R. (2012). Nitrogen and phosphorus effects on water use efficiency of spring
753 wheat grown in a semi-arid region of the Canadian prairies. *Canadian Journal of Soil*
754 *Science*, 92(4), 573–587. doi:10.4141/cjss2011-055
755
- 756 Legendre, P. & Legendre, L. (2012). *Numerical Ecology*. 3rd edn. Elsevier, Amsterdam.
757
- 758 Lavorel, S., & Garnier, E. (2002) Predicting changes in community composition and
759 ecosystem functioning from plant traits: revisiting the Holy Grail. *Functional Ecology* 16,
760 545–556.
761
- 762 Liu, X., N.G. Swenson, D. Lin, X. Mi, M.N. Umana, B. Schmid, & K. Ma. (2016)
763 Linking individual-level traits to tree growth in a subtropical forest. *Ecology* 97, 2396-
764 2405. doi: 10.1002/ecy.1445
765

- 766 McGill, B. J., Enquist, B. J., Weiher, E., & Westoby, M. (2006). Rebuilding community
767 ecology from functional traits. *Trends in Ecology and Evolution*, 21(4), 178–185.
768 doi:10.1016/j.tree.2006.02.002
769
- 770 Medeiros, C. D., Scoffoni, C., John, G. P., Bartlett, M. K., Inman-Narahari, F., Ostertag,
771 R., ... , and Sack, L. (2018). An extensive suite of functional traits distinguishes Hawaiian
772 wet and dry forests and enables prediction of species vital rates. *Functional Ecology* 33,
773 712-734. doi: 10.1111/1365-2435.13229
774
- 775 Niinemets, Ü., Portsmouth, & D., Tobias. (2007). Leaf shape and venation pattern alter
776 the support investments within leaf lamina in temperate species: a neglected source of
777 leaf physiological differentiation?. *Functional Ecology*, 21: 28-40.
778
- 779 Niklas, K. J., & Enquist, B. J. (2001). Invariant scaling relationship for interspecific plant
780 biomass production rates and body size. *Proc. Natl. Acad. Sci.* 98, 2922-2927
781
- 782 Pacala, S., & Silander, J. A. (1985). Neighbourhood Models of Plant Population
783 Dynamics. I. Single-Species Models of Annuals. *The American Naturalist*, 125(3), 385-
784 411.
785
- 786 Paine, C. E. T., Amisshah, L., Auge, H., Baraloto, C., Baruffol, M., Bourland, N., ...
787 Hector, A. (2015). Globally, functional traits are weak predictors of juvenile tree growth,
788 and we do not know why. *Journal of Ecology*, 103(4), 978–989. doi:10.1111/1365-
789 2745.12401
790
- 791 Poorter, H. (1989). Interspecific variation in relative growth rate: on ecological causes
792 and physiological consequences, In Lambers, H., Cambridge, M. L., Konings, H., and
793 Pons, T. L (Eds.), *Causes and consequences of variation in growth rate and productivity*
794 *in higher plants* (pp. 45-68). The Hague, the Netherlands: SPB Academic Publishing.
795

- 796 Poorter, H. & Villar, R. (1997). The Fate of Acquired Carbon in Plants: Chemical
797 Composition and Construction Costs, In F. A. Bazzaz and J. Grace (Eds.), *Plant*
798 *Resource Allocation* (pp. 39-72). San Diego: Academic Press.
799
- 800 Poorter, H. & van der Werf, A. (1998). Is inherent variation in RGR determined by LAR
801 at low irradiance and by NAR at high irradiance? A review of herbaceous species. In
802 Lambers, H., Poorter, H., van Vuuren, M.M.I., Leiden (Eds.), *Inherent variation in plant*
803 *growth. Physiological mechanisms and ecological consequences* (pp.309-336). Leiden,
804 The Netherlands: Backhuys Publishers.
- 805 Poorter, L., Bongers, F., Sterck, F. J., & Wöll, H. (2005). Beyond the regeneration phase:
806 Differentiation of height-light trajectories among tropical tree species. *Journal of*
807 *Ecology*, 93(2), 256–267. doi:10.1111/j.1365-2745.2004.00956.x
808
- 809 Poorter, L., Wright, S. J., Paz, H., Ackerly, D. D., Condit, R., Ibarra-Manríquez, G., ...
810 Wright, I. J. (2008). Are functional traits good predictors of demographic rates? Evidence
811 from five neotropical forests. *Ecology*, 89(7), 1908–1920. doi:10.1890/07-0207.1
812
- 813 Rees, M. (1996). Evolutionary ecology of seed dormancy and seed size. *Philosophical*
814 *Transactions of the Royal Society B: Biological Sciences*, 351(1345).
815
- 816 Reich, P. B., Walters, M. B., & Ellsworth, D. S. (1997). From tropics to tundra: Global
817 convergence in plant functioning. *Proceedings of the National Academy of Sciences*,
818 94(25), 13730–13734. doi:10.1073/pnas.94.25.13730
- 819 Resa, M. d.I.A., Emir, B., & Cabrera, J. (2017). qrmix: Quantile Regression Mixture
820 Models. R package version 0.9.0. <https://CRAN.R-project.org/package=qrmix>
821
- 822 Ryan, M. G., D. Binkley, and J. H. Fownes. (1997). Age-related decline in forest
823 productivity: pattern and process. *Adv. Ecol. Res.* 27:213–262.
824
- 825 Sack, L., & Frole, K. (2006). Leaf structural diversity is related to hydraulic capacity in
826 tropical rain forest trees. *Ecology*, 87(2), 483–491. doi:10.1890/05-0710

- 827
828 Sack, L., & Scoffoni, C. (2013). Leaf venation: structure, function, development,
829 evolution, ecology and applications in the past, present and future. *New Phytologist*, 198:
830 983–1000. doi: 10.1111/nph.12253
831
- 832 Sack, L., Scoffoni, C., John, G. P., Poorter, H., Mason, C. M., Mendez-Alonzo, R., &
833 Donovan, L. A. (2013). How do leaf veins influence the worldwide leaf economic
834 spectrum? Review and synthesis. *Journal of Experimental Botany*, 64(13), 4053–4080.
835 doi:10.1093/jxb/ert316
836
- 837 Santiago, L. S., Goldstein, G., Meinzer, F. C., Fisher, J. B., Machado, K., Woodruff, D.,
838 & Jones, T. (2004). Leaf photosynthetic traits scale with hydraulic conductivity and wood
839 density in Panamanian forest canopy trees. *Oecologia*, 140(4), 543–550.
840 doi:10.1007/s00442-004-1624-1
841
- 842 Santiago, L. S., De Guzman, M. E., Baraloto, C., Vogenberg, J. E., Brodie, M., Hérault,
843 B., Fortunel, C., & Bonal, D. (2018). Coordination and trade-offs among hydraulic
844 safety, efficiency and drought avoidance traits in Amazonian rainforest canopy tree
845 species. *New Phytologist*, 18, 1015-1024.
846
- 847 Seibt, U., Rajabi, A., Griffiths, H., & Berry, J. A. (2008). Carbon isotopes and water use
848 efficiency: Sense and sensitivity. *Oecologia*, 155(3), 441–454. doi:10.1007/s00442-007-
849 0932-7
850
- 851 Song, C. J., Ma, K. M., Qu, L. Y., Liu, Y., Xu, X. L., Fu, B. J., & Zhong, J. F. (2010).
852 Interactive effects of water, nitrogen and phosphorus on the growth, biomass partitioning
853 and water-use efficiency of *Bauhinia faberi* seedlings. *Journal of Arid Environments*,
854 74(9), 1003–1012. doi:10.1016/j.jaridenv.2010.02.003
855
- 856 Swenson, N.G., J.C. Stegen, S.J. Davies, D.L. Erickson, J. Forero-Montana, A.H.
857 Hurlbert, W.J., ..., J.K. Zimmerman. (2012). Temporal turnover in the composition of

- 858 tropical tree communities: functional determinism and phylogenetic stochasticity.
859 Ecology 93, 490-499. doi: 10.1890/11-1180.1
860
- 861 Swenson, N.G., Umana, M.N. (2015) Data from: Interspecific functional convergence
862 and divergence and intraspecific negative density dependence underlie the seed-to-
863 seedling transition in tropical trees. Dryad Digital Repository. doi: 10.5061/dryad.j2r53
864
- 865 Swenson, N. G., Iida, Y., Howe, R., Wolf, A., Umaña, M. N., Petprakob, K., Turner, B.
866 L., & Ma, K. (2017). Tree co-occurrence and transcriptomic response to drought. Nature
867 Communications, 8(1), 1–9. doi:10.1038/s41467-017-02034-w
868
- 869 Swenson, N.G., Iida, Y., & Rubio, V.E. (2020), Data from: Improving predictions of
870 tropical tree survival and growth by incorporating measurements of whole leaf allocation,
871 Dryad Digital Repository. <https://doi.org/10.5061/dryad.4mw6m908c>
872
- 873 Symonds, M. R. E. & A. Moussalli. (2011). A brief guide to model selection, multimodel
874 inference and model averaging in behavioural ecology using Akaike’s information
875 criterion. Behavioral Ecology and Sociobiology, 65, 13-21.
876
- 877 Umaña, M. N., Forero-Montaña, J., Muscarella, R., Nytch, C. J., Thompson, J., Uriarte,
878 M.,..., Swenson, N.G. (2015) Interspecific functional convergence and divergence and
879 intraspecific negative density dependence underlie the seed-to-seedling transition in
880 tropical trees. The American Naturalist 187(1), 99-109. doi: 10.1086/684174
881
- 882 Umaña, M. N., Zhang, C., Cao, M., Lin, L., & Swenson, N. G. (2017). A core-transient
883 framework for trait-based community ecology: an example from a tropical tree seedling
884 community. Ecology Letters, 20, 619-628.
885
- 886 Uriarte, M., Canham, C. D., Thompson, J., & Zimmerman, J. K. (2004). A
887 neighbourhood analysis of tree growth and survival in a hurricane-driven tropical forest.
888 Ecological monographs, 74, 591-614

889

890 Uriarte, M., Swenson, N. G., Chazdon, R. L., Comita, L. S., Kress, W. J., Erickson, D.,
891 Forero-Montaña, J., Zimmerman, J. K., & Thompson, J. (2010). Trait similarity, shared
892 ancestry and the structure of neighbourhood interactions in a subtropical wet forest:
893 implications for community assembly. *Ecology Letters*, 13, 1503-1514.

894

895 Walker, L. R., N. V. L. Brokaw, D. J. Lodge, and R. B. Waide, editors. 1991. Special
896 issue. Ecosystem, plant, and animal responses to hurricanes in the Caribbean. *Biotropica*,
897 23, 313-521.

898

899 Weiner, J. (1990) Asymmetric competition in plant populations. *Trends in Ecology and*
900 *Evolution*, 5, 360–364.

901

902 Westoby, M. (1998). A leaf-height-seed (LHS) plant ecology strategy scheme. *Plant and*
903 *Soil*, 199, 213-227.

904

905 Westoby, M., Falster, D. S., Moles, A. T., Vesk, P. A., & Wright, I. J. (2002). Plant
906 Ecological Strategies: some leading dimensions of variation between species. *Annual*
907 *Review of Ecology and Systematics*, 33, 125–159.

908

909 Worthy, S.J., & N. G. Swenson. (2019). Functional perspectives on tropical tree
910 demography and forest dynamics. *Ecological Processes*, 8, 1.

911

912 Wright, I. J., Reich, P. B., Westoby, M., Ackerly, D. D., Baruch, Z., Bongers, F.,...,
913 Villar, R. (2004). The worldwide leaf economics spectrum. *Nature*, 428(6985), 821–827.
914 doi:10.1038/nature02403

915

916 Wright, S. J., Kitajima, K., Kraft, N. J. B., Reich, P. B., Wright, I. J., Bunker, D. E., ...,
917 Zanne, A. E. (2010). Functional traits and the growth — mortality trade-off in tropical
918 trees. *Ecology*, 91(12), 3664–3674. doi:10.1890/09-2335.1

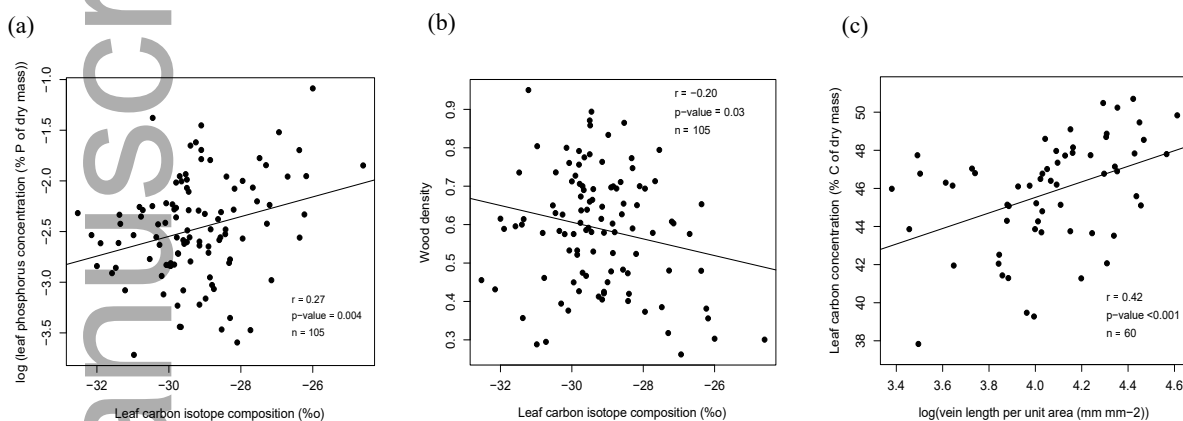
919

- 920 Yan, Y. (2016). MLmetrics: Machine Learning Evaluation Metrics. R package version
921 1.1.1. <https://CRAN.R-project.org/package=MLmetrics>
922
- 923 Yang, J., Cao, M., & Swenson, N. G. (2018). Why functional traits do not predict tree
924 demographic rates. *Trends in Ecology and Evolution*, 33(5), 326–336.
925 doi:10.1016/j.tree.2018.03.003
926
- 927 Yang, J., Song, X., Cao, M., Deng, X., Zhang, W., Yang, X., & Swenson, N. G. (2020).
928 On the modeling of tropical tree growth: the importance of intra-specific trait variation,
929 non-linear functions and phenotypic integration. *Annals of Botany*.
930 doi:10.1093/aob/mcaa085
931
- 932 Zambrano, J., Marchand, P., & Swenson, N. G. (2017). Local neighbourhood and
933 regional climatic contexts interact to explain tree performance. *Proc. R. Soc. B* 284:
934 20170523. doi:10.1098/rspb.2017.0523
935
- 936 Zambrano, J., Y. Iida, R. Howe, L. Lin, M.N. Umana, A. Wolf, Worthy, S. J., Swenson,
937 N. G. (2017). Neighbourhood defense gene similarity effects on tree performance: a
938 community transcriptomic approach. *Journal of Ecology* 105:616-626. doi:
939 10.1111/1365-2745.12765
940
- 941 Zambrano, J., Fagan, W. F., Worthy, S. J., Thompson, J., Uriarte, M., Zimmerman, J. K.,
942 Umaña, M. N., & Swenson, N. G. (2019). Tree crown overlap improves predictions of
943 the functional neighbourhood effects on tree survival and growth. *Journal of Ecology*
944 107: 887-900.
945
- 946 Zambrano, J., Beckman, N. G., Marchand, P., Thompson, J., Uriarte, M., Zimmerman, J.
947 K., Umaña, M. N., & Swenson, N. G. (2020). The scale dependency of trait-based tree
948 neighbourhood models. *Journal of Vegetation Science* 00: 1-13.
949

950 Zimmerman J. (2010). Census of species, diameter and location at the Luquillo Forest
 951 Dynamics Plot (LFDP), Puerto Rico. Environmental Data Initiative.
 952 <https://doi.org/10.6073/pasta/6061298660b4ceb806ba49805a950646>. Dataset accessed
 953 2/02/2020.

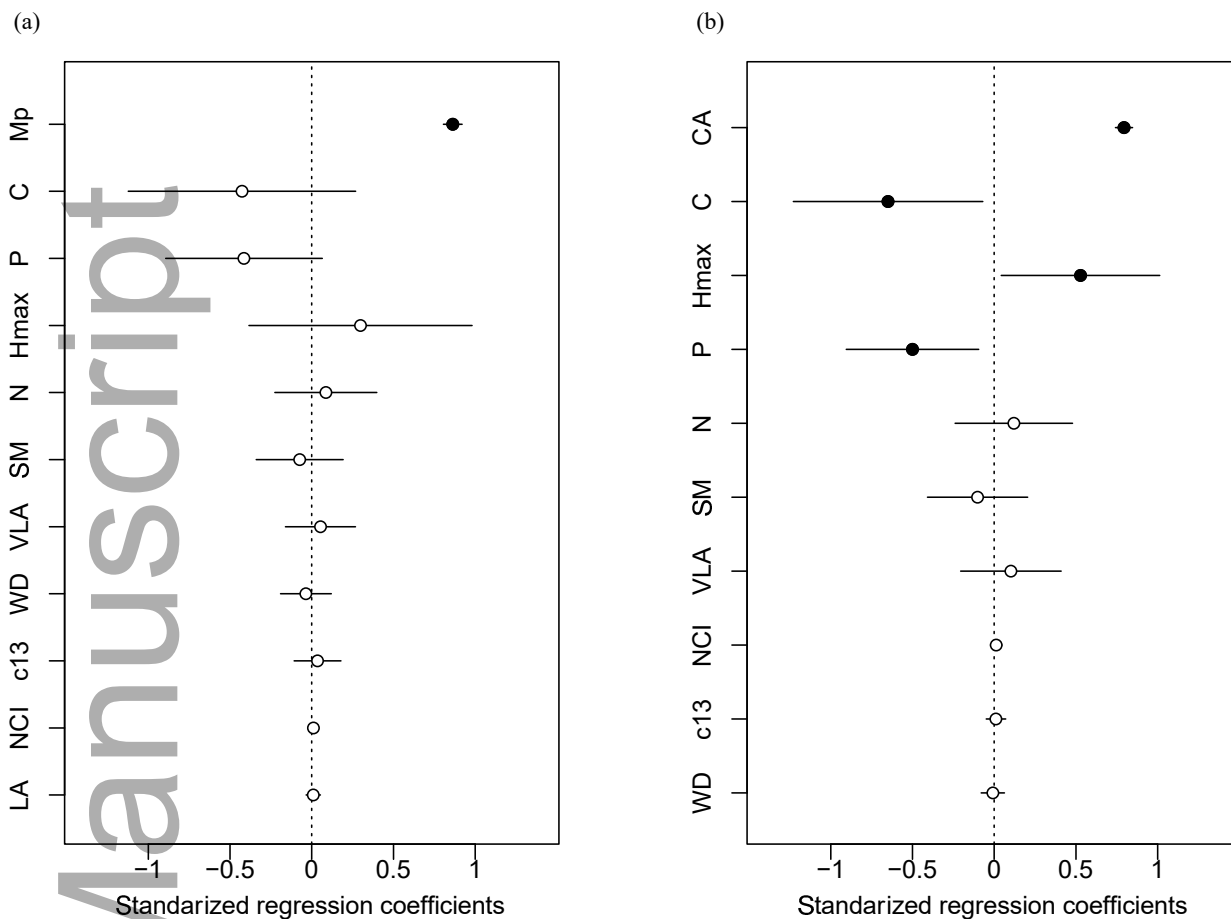
954
 955
 956

FIGURES



957
 958
 959
 960
 961
 962
 963

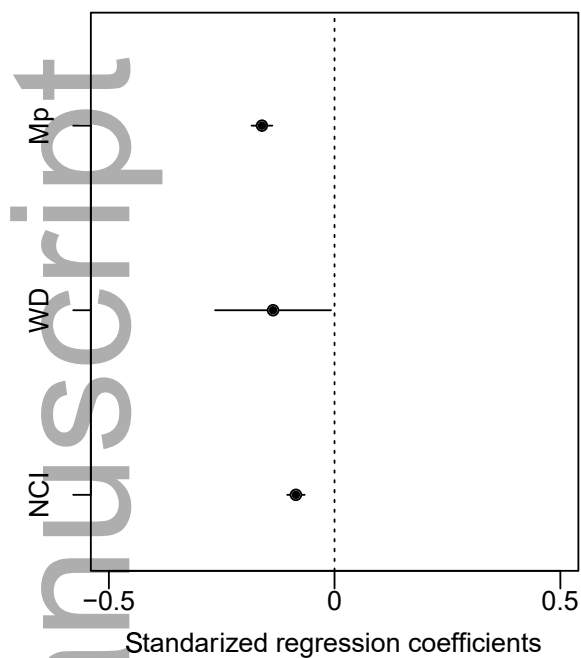
Figure 1. (a) Correlation between leaf carbon isotope composition and leaf phosphorus concentration. (b) Correlation between leaf carbon isotope composition and wood density. (c) Correlation between vein length per unit area (VLA) and leaf carbon concentration. The Pearson correlation coefficient (r), sample size (n), and p -value are shown for each graph.



964

965 **Figure 2.** Standardized regression coefficients for the averaged survival models. Two
 966 averaged models were applied: (a) a model including photosynthetic mass (M_p) and traits;
 967 and (b) a model including photosynthetic crown area (CA) and traits. Refer to Table 1 for
 968 abbreviations. Variables are displayed in order of importance. Lines represent 95%
 969 confidence intervals, while circles represent the model estimated value. Open circles are
 970 non-significant effect, and filled black circles represent a significant parameter at $\alpha =$
 971 0.05. Refer to Table 4 for details.

972



973

974 **Figure 3.** (a) Model standardized regression coefficient for the averaged growth model.
 975 Variables are displayed in order of importance. Refer to Table 1 for abbreviations. Lines
 976 represent 95% confidence intervals, while the circles represent the model estimated value.
 977 Filled black circles represent a significant effect. Standardization was performed by log-
 978 transforming and scaling (z-scoring, subtracting the mean and dividing by the standard
 979 deviation) the variables. Refer to Table 6 for details.

980

981

982

983

984

985 **TABLES**

986 **Table 1.** Soft- and hard-traits considered as potential predictors of tree survival and
 987 growth rates.

Soft-traits

| | | |
|---|-------------------------------|--|
| Commonly measured but weakly correlated or not correlated at all with important physiological rates | Leaf phosphorus concentration | P (%P) |
| | Leaf carbon concentration | C (%C) |
| | Leaf nitrogen concentration | N (%N) |
| | Wood density | WD |
| | Leaf area | LA (cm ²) |
| | Specific leaf area | SLA (cm ² g ⁻¹) |
| | Maximum tree height | H (m) |
| | Seed dry mass | SM (g) |

Hard-traits

| | | |
|--|--|----------------------------|
| Difficult to measure but closely linked to physiological processes of interest | Stable leaf carbon isotope composition | $\delta^{13}\text{C}$ (‰) |
| | Vein length per unit area | VLA (mm mm ⁻²) |

988

989

990 **Table 2.** Survival (S) and growth (RGR) models. The table shows the models compared
 991 to determine whether including total photosynthetic mass estimates (M_p) outperformed
 992 models that included the components of M_p by themselves. Also included were an
 993 intercept (β_0), crown area (CA), initial diameter at breast height (dbh), and leaf mass per
 994 area (LMA). Variables that are significant in a model are bolded. Moreover, Akaike's
 995 value (AIC), ΔAIC ($\text{AIC}_i - \text{AIC}_{\min}$), Akaike weights (w_i), and Cross-Validation loss (C-V
 996 loss) are shown for each model. Lower Cross-Validation loss (C-V loss) values are
 997 underlined showing the model with best goodness of fit and higher probability of being
 998 the best model.

999

| Model | AIC | ΔAIC | w_i | C-V loss |
|---------------------------------|---------|--------------------|--------|-----------------|
| $S \sim \beta_0 + M_p$ | 16049.8 | 0 | 0.495 | <u>0.453323</u> |
| $S \sim \beta_0 + CA$ | 16058.6 | 0 | 0.498 | <u>0.453323</u> |
| $S \sim \beta_0 + dbh$ | 16049.8 | 8.8 | 0.006 | 0.453670 |
| $S \sim \beta_0 + LMA$ | 17063.6 | 1013.77 | <0.001 | 0.485296 |
| $\text{RGR} \sim \beta_0 + M_p$ | 28388.4 | 0 | 0.615 | <u>0.281690</u> |

| | | | | |
|-----------------------|---------|-------|--------|----------|
| RGR ~ $\beta_0 + CA$ | 28389.4 | 1 | 0.381 | 0.281712 |
| RGR ~ $\beta_0 + dbh$ | 28398.5 | 10.1 | 0.004 | 0.281812 |
| RGR ~ $\beta_0 + LMA$ | 28548.7 | 160.3 | <0.001 | 0.282589 |

1000

1001

1002 **Table 3.** Survival (S) models that include total photosynthetic mass (M_p) or crown area1003 (CA). The table shows the set of models for survival with $\Delta AIC \leq 2$ that include the1004 intercept (β_0), and soft- and hard-traits (refer to Table 1 for abbreviations). Moreover,1005 Akaike's value (AIC), ΔAIC ($AIC_i - AIC_{min}$), Akaike weights (w_i), and Cross-Validation

1006 loss (C-V loss) are shown for each model.

| Model | AIC | ΔAIC | w_i | C-V loss |
|---|---------|--------------|-------|----------|
| S ~ $\beta_0 + M_p + C + Hmax + P$ | 16047.6 | 0 | 0.095 | 0.453325 |
| S ~ $\beta_0 + M_p + C + Hmax + P + N + SM + VLA$ | 16047.7 | 0.1 | 0.089 | 0.453337 |
| S ~ $\beta_0 + M_p + C + Hmax + P + NCI$ | 16048.1 | 0.4 | 0.076 | 0.453288 |
| S ~ $\beta_0 + M_p + C + Hmax + N + P + SM + NCI + VLA$ | 16048.2 | 0.5 | 0.073 | 0.453301 |
| S ~ $\beta_0 + M_p + P$ | 16048.4 | 0.8 | 0.065 | 0.453317 |
| S ~ $\beta_0 + M_p + C + P$ | 16048.5 | 0.9 | 0.061 | 0.453324 |
| S ~ $\beta_0 + M_p + C + Hmax + P + c13$ | 16048.7 | 1.0 | 0.056 | 0.453331 |
| S ~ $\beta_0 + M_p + P + NCI$ | 16048.8 | 1.2 | 0.053 | 0.453281 |
| S ~ $\beta_0 + M_p + C + Hmax + N + P + SM + VLA + c13$ | 16048.9 | 1.3 | 0.051 | 0.453344 |
| S ~ $\beta_0 + M_p + C + P + NCI$ | 16048.9 | 1.3 | 0.049 | 0.453287 |
| S ~ $\beta_0 + M_p + Hmax + P$ | 16049.0 | 1.3 | 0.048 | 0.453314 |
| S ~ $\beta_0 + M_p + C + P + wsg$ | 16049.1 | 1.4 | 0.046 | 0.453325 |
| S ~ $\beta_0 + M_p + C + Hmax + P + NCI + c13$ | 16049.1 | 1.5 | 0.045 | 0.453294 |
| S ~ $\beta_0 + M_p + C + Hmax + P + wsg$ | 16049.2 | 1.6 | 0.042 | 0.453327 |
| S ~ $\beta_0 + M_p + Hmax + P + NCI$ | 16049.4 | 1.8 | 0.039 | 0.453277 |
| S ~ $\beta_0 + M_p + P + LA$ | 16049.4 | 1.8 | 0.039 | 0.453311 |
| S ~ $\beta_0 + M_p + C + P + NCI + wsg$ | 16049.5 | 1.9 | 0.037 | 0.453289 |
| S ~ $\beta_0 + M_p + C + c13$ | 16049.6 | 2 | 0.035 | 0.453336 |
| S ~ $\beta_0 + CA + C + Hmax + P$ | 16045.0 | 0 | 0.268 | 0.453334 |
| S ~ $\beta_0 + CA + C + Hmax + P + NCI$ | 16045.4 | 0.4 | 0.217 | 0.453298 |
| S ~ $\beta_0 + CA + C + Hmax + P + N + SM + VLA$ | 16046.0 | 1.0 | 0.163 | 0.453347 |
| S ~ $\beta_0 + CA + C + Hmax + N + P + SM + NCI + VLA$ | 16046.4 | 1 | 0.134 | 0.453311 |
| S ~ $\beta_0 + CA + C + Hmax + P + c13$ | 16046.7 | 1.7 | 0.115 | 0.453336 |
| S ~ $\beta_0 + CA + C + Hmax + P + wsg$ | 16046.9 | 1.9 | 0.104 | 0.453335 |

1007

1008

1009

1010 **Table 4.** Average survival (S) models that include total photosynthetic mass (Mp) or crown
 1011 area (CA), and soft- and hard-traits (refer to Table 1 for abbreviations). Variables are
 1012 displayed in order of importance. Also included are the unconditional (model selection
 1013 uncertainty not conditional in any particular model from the set) sampling standard error (\widehat{SE}),
 1014 unconditional confidence intervals (Lower CI and Upper CI), and absolute Wald
 1015 values are shown for each variable.

1016

| Variable | Estimate | \widehat{SE} | Lower CI | Upper CI | Wald Z |
|--|----------|----------------|----------|----------|--------|
| S ~ β_0 + Mp + C + Hmax + P + N + SM + VLA + NCI + c13 + WD + LA | | | | | |
| Mp | 0.863 | 0.029 | 0.806 | 0.919 | 29.8 |
| C | -0.427 | 0.355 | -1.122 | 0.269 | 1.20 |
| H | 0.298 | 0.348 | -0.384 | 0.980 | 0.86 |
| P | -0.415 | 0.244 | -0.894 | 0.064 | 1.70 |
| N | 0.086 | 0.159 | -0.225 | 0.398 | 0.54 |
| SM | -0.073 | 0.136 | -0.339 | 0.192 | 0.54 |
| VLA | 0.053 | 0.109 | -0.160 | 0.267 | 0.49 |
| NCI | 0.010 | 0.017 | -0.023 | 0.043 | 0.61 |
| c13 | 0.035 | 0.073 | -0.108 | 0.178 | 0.48 |
| WD | -0.036 | 0.079 | -0.191 | 0.119 | 0.45 |
| LA | 0.010 | 0.022 | -0.034 | 0.053 | 0.43 |
| S ~ β_0 + CA + C + Hmax + P + N + SM + VLA + NCI + c13 + WD | | | | | |
| CA | 0.794 | 0.027 | 0.742 | 0.846 | 29.8 |
| C | -0.649 | 0.296 | -1.229 | -0.070 | 2.20 |
| H | 0.528 | 0.247 | 0.043 | 1.013 | 2.13 |
| P | -0.500 | 0.206 | -0.904 | -0.096 | 2.42 |
| N | 0.120 | 0.183 | -0.239 | 0.479 | 0.66 |
| SM | -0.102 | 0.156 | -0.408 | 0.204 | 0.65 |
| VLA | 0.102 | 0.157 | -0.205 | 0.409 | 0.65 |
| NCI | 0.012 | 0.018 | -0.023 | 0.047 | 0.69 |
| c13 | 0.010 | 0.030 | -0.049 | 0.070 | 0.34 |

WD -0.009 0.036 -0.080 0.063 0.24

1017

1018

1019 **Table 5.** Growth (RGR) models. The table shows the set of models with indiscernible

1020 $\Delta\text{AIC} \leq 2$ that include intercept (β_0) and traits (refer to Table 1 for abbreviations).

1021 Moreover, Akaike value (AIC), ΔAIC ($\text{AIC}_i - \text{AIC}_{\min}$), Akaike weights (w_i), and Cross-

1022 Validation loss (C-V loss) are shown for each model.

| Model | AIC | ΔAIC | wi | C-V loss |
|--|---------|--------------------|------|----------|
| RGR ~ $\beta_0 + \text{Mp} + \text{WD} + \text{NCI}$ | 28321.7 | 0 | 0.67 | 0.281006 |
| RGR ~ $\beta_0 + \text{Mp} + \text{NCI}$ | 28323.1 | 1.4 | 0.33 | 0.281043 |

1023

1024

1025 **Table 6.** Average growth (RGR) models that include total photosynthetic mass (Mp) and

1026 soft- and hard-traits (refer to Table 1 for abbreviations). Variables are displayed in order

1027 of importance. Also included are the unconditional (model selection uncertainty not

1028 conditional in any particular model from the set) sampling standard error (\hat{SE}),

1029 unconditional confidence intervals (Lower CI and Upper CI), and absolute Wald values are

1030 shown for each variable.

| Variable | Estimate | \hat{SE} | Lower CI | Upper CI | Wald Z |
|--|----------|------------|----------|----------|--------|
| RGR ~ $\beta_0 + \text{Mp} + \text{WD} + \text{NCI}$ | | | | | |
| Mp | -0.161 | 0.012 | -0.184 | -0.138 | 13.71 |
| WD | -0.136 | 0.065 | -0.265 | -0.008 | 2.08 |
| NCI | -0.086 | 0.010 | -0.105 | -0.066 | 8.72 |

1031